


# N-terminal heterogeneity of parenchymal and vascular amyloid- $\beta$ deposits in Alzheimer's disease

S. Zampar\*, H. W. Klafki\*, K. Sritharen\*, T. A. Bayer\*, J. Wiltfang\*†‡, A. Rostagno§, J. Ghiso§¶, L. A. Miles\*\* and O. Wirths\* 

\*Department of Psychiatry and Psychotherapy, University Medical Center (UMG), Georg-August-University, Göttingen, Germany, †Neurosciences and Signaling Group, Department of Medical Sciences, Institute of Biomedicine (iBiMED), University of Aveiro, Aveiro, Portugal, ‡German Center for Neurodegenerative Diseases (DZNE), Göttingen, Germany, §Pathology, ¶Psychiatry, New York University School of Medicine, New York, NY, USA and \*\*St. Vincent's Institute of Medical Research, Fitzroy, VIC, Australia

S. Zampar, H. W. Klafki, K. Sritharen, T. A. Bayer, J. Wiltfang, A. Rostagno, J. Ghiso, L. A. Miles and O. Wirths (2020) *Neuropathology and Applied Neurobiology* 46, 673–685

## N-terminal heterogeneity of parenchymal and vascular amyloid- $\beta$ deposits in Alzheimer's disease

**Aims:** The deposition of amyloid- $\beta$  (A $\beta$ ) peptides in the form of extracellular plaques in the brain represents one of the classical hallmarks of Alzheimer's disease (AD). In addition to 'full-length' A $\beta$  starting with aspartic acid (Asp-1), considerable amounts of various shorter, N-terminally truncated A $\beta$  peptides have been identified by mass spectrometry in autopsy samples from individuals with AD. **Methods:** Selectivity of several antibodies detecting full-length, total or N-terminally truncated A $\beta$  species has been characterized with capillary isoelectric focusing assays using a set of synthetic A $\beta$  peptides comprising different N-termini. We further assessed the N-terminal heterogeneity of extracellular and vascular A $\beta$  peptide deposits in the human brain by performing immunohistochemical analyses using sporadic AD cases with antibodies targeting different N-terminal residues, including the biosimilar antibodies Bapineuzumab and Crenezumab. **Results:** While antibodies selectively

recognizing A $\beta_{1-x}$  showed a much weaker staining of extracellular plaques and tended to accentuate cerebrovascular amyloid deposits, antibodies detecting A $\beta$  starting with phenylalanine at position 4 of the A $\beta$  sequence showed abundant amyloid plaque immunoreactivity in the brain parenchyma. The biosimilar antibody Bapineuzumab recognized A $\beta$  starting at Asp-1 and demonstrated abundant immunoreactivity in AD brains. **Discussion:** In contrast to other studied A $\beta_{1-x}$ -specific antibodies, Bapineuzumab displayed stronger immunoreactivity on fixed tissue samples than with sodium dodecyl sulfate-denatured samples on Western blots. This suggests conformational preferences of this antibody. The diverse composition of plaques and vascular deposits stresses the importance of understanding the roles of various A $\beta$  variants during disease development and progression in order to generate appropriate target-developed therapies.

**Keywords:** Alzheimer disease, amyloid, N-terminal truncation, capillary isoelectric focusing immunoassay, antibody, Abeta

## Introduction

The deposition of amyloid- $\beta$  (A $\beta$ ) peptides in the form of extracellular plaques in the brain parenchyma is one of the characteristic neuropathological features of

Correspondence: Oliver Wirths, Department of Psychiatry, University Medical Center Göttingen, Von-Siebold-Str. 5, 37075 Goettingen, Germany. Tel: +49-551-3965669; Fax: +49-551-3912655; E-mail: owirths@gwdg.de

Alzheimer's disease (AD). These A $\beta$  peptides are derived from the larger amyloid precursor protein (APP) and generated by sequential proteolytic cleavage events carried out by the so-called  $\beta$ - and  $\gamma$ -secretases [1]. The A $\beta$  cascade hypothesis postulates a central role of A $\beta$  in the disease process [2] and is supported by genetic findings in familial early onset AD (EOAD) cases. In these patients, autosomal dominant mutations in the genes encoding APP or presenilins (PSEN) have been identified which inevitably lead to EOAD [3,4]. On the other hand, a lack of a robust correlation between extracellular amyloid pathology and the cognitive status of AD patients has questioned the validity of this concept [5,6]. The recent failures of several clinical trials employing therapeutic antibodies directed against A $\beta$  peptides fuelled additional scepticism [7-13]. A $\beta$  immunoprecipitation combined with matrix-assisted laser desorption/ionization time-of-flight (TOF) mass spectrometry in brain tissue samples from AD subjects revealed the presence of a variety of A $\beta$  peptides with differences in length due to N- and C-terminal truncations [14-20]. A shortened N-terminus and a longer C-terminus appear to facilitate peptide aggregation into beta-sheet fibrils, and thereby increase their neurotoxicity as compared to full-length A $\beta$  peptides. In addition to N- or C-terminal truncations, post-translational protein modifications such as the formation of N-terminal pyroglutamate residues (A $\beta$ <sub>PE3-x</sub>, A $\beta$ <sub>PE11-x</sub>) [21,22] or A $\beta$  peptide phosphorylation [23,24] have been reported. Furthermore, N-truncated A $\beta$  variants may act as initiators of amyloid deposition [25]. Analysis of amyloid core preparations revealed the presence of A $\beta$  peptides beginning with every residue between aspartic acid (Asp)-1 and glutamate (Glu)-11, but with major signals for peptides starting with phenylalanine (Phe)-4, serine (Ser)-8 and Glu-11 [26]. A $\beta$ <sub>4-42</sub> has been detected by surface-enhanced laser desorption/ionization TOF (SELDI-TOF) mass spectrometry with strong signals in *post mortem* brain samples from aged controls, patients with vascular dementia and AD patients [27]. Among the different N-truncated A $\beta$  forms, A $\beta$ <sub>4-42</sub> was found to be the major N-truncated A $\beta$  species in parenchymal A $\beta$ -plaques [28]. In contrast, cerebrovascular amyloid was reported by Miller *et al.* to contain mainly A $\beta$  peptides starting with residues 1 or 2 [26]. However, more recently also A $\beta$ <sub>4-40</sub> or A $\beta$ <sub>4-42</sub> peptides have been described in cases with congophilic amyloid angiopathy (CAA) or AD + CAA [16]. The conformational/aggregation state of A $\beta$  peptides is an

additional aspect to take into consideration when discussing the validity of A $\beta$  as a therapeutic target. Besides the classical 'Amyloid Hypothesis' that sees amyloid deposition as a critical pathogenic event in AD [2], the role of soluble A $\beta$  oligomers as key actors in synaptic dysfunction, neuron loss and memory deficits has grown in favour. Today, it is generally accepted that the apparently pathologically inert amyloid fibrils, which are found in plaques, originate from a nearly irreversible aggregation of monomeric A $\beta$  peptides through toxic protofibrillar intermediates [29]. The function of amyloid plaques in this scenario is still a matter of controversial debates, whether they act as a reservoir of toxic amyloid oligomers or possess buffering properties [30]. While several preclinical immunotherapy studies employing anti-A $\beta$  antibodies have demonstrated beneficial effects with regard to reduced extracellular plaque pathology [31,32], others also reported that passive immunization might cause severe vascular alterations such as increased frequency of haemorrhages [33,34]. Considering the controversial outcome of the immunotherapies in AD so far, a better understanding of the spatial localization or distribution of specific A $\beta$  variants (e.g. N-terminal truncated or C-terminal elongated), and ultimately their role in the aetiology of the disease, is of high importance. Moreover, given that different A $\beta$  conformation and/or aggregation states might have different roles in the pathology, the affinity of antibodies used in immunotherapy to bind to the different A $\beta$  states is an additional crucial characteristic to take into consideration. In this study, a variety of antibodies detecting N-terminal A $\beta$  variants were characterized in detail and used to assess the N-terminal heterogeneity of extracellular and vascular A $\beta$  peptide deposits in human brain samples.

## Materials and methods

### Antibody characterization by capillary isoelectric focusing immunoassay

In order to evaluate the selectivity of a set of different antibodies detecting either full-length or N-terminal truncated variants of A $\beta$  ending at position 40 as well as 42, a capillary isoelectric focusing immunoassay (CIEF-immunoassay) was employed as published previously [35,36]. In brief, synthetic A $\beta$  peptides with different N-termini were separated on a Peggy Sue device (Protein Simple, San

Jose, CA, USA) by isoelectric focusing in microcapillaries. Next, the detection was carried out using mouse monoclonal antibodies 80C2 (#218231, Synaptic Systems, Goettingen, Germany, 20  $\mu$ g/ml) and 82E1 (IBL International, Hamburg, Germany, 20  $\mu$ g/ml), both detecting full-length A $\beta$  starting with Asp-1, antibody 18H6 (1.9  $\mu$ g/ml) [20] detecting truncated A $\beta$  starting with Phe-4 and the generic A $\beta$  antibody 4G8 (BioLegend, San Diego, CA, USA, 2  $\mu$ g/ml). The rabbit polyclonal generic antibody 24311 [37] and the humanized murine monoclonal biosimilar antibodies of Bapineuzumab [38] (14  $\mu$ g/ml) and Crenezumab [38] (17  $\mu$ g/ml), which have been used in clinical trials, were also used in the assay. The synthetic A $\beta$  peptides A $\beta$ <sub>1–40/42</sub>, A $\beta$ <sub>2–40/42</sub>, A $\beta$ <sub>3–40/42</sub>, pyroglutamate A $\beta$ <sub>pE3–40/42</sub>, A $\beta$ <sub>4–40/42</sub>, A $\beta$ <sub>5–40</sub> and A $\beta$ <sub>11–40</sub> were purchased from AnaSpec (Fremont, CA, USA). The synthesis of A $\beta$ <sub>–3–40/42</sub> (corresponding to APP669–711/713) has been described previously [39] (generous gift of Dr H.-J. Knölker, Dresden). Peptide stock solutions (1 mg/ml) were prepared in DMSO or, in the case of A $\beta$ <sub>pE3–40</sub>, in 0.1% NH<sub>3</sub>(aq) (~0.1% NH<sub>3</sub>(w/v)) and stored at –80°C. Working aliquots were thawed only once. Following further dilution in 20 mM bicine pH 7.6, 0.6% 3-[(3-cholamidopropyl) dimethylammonio]-1-propanesulphonate (CHAPS), peptides were mixed in a 1:4 ratio with G2 Premix containing a pH5–pH8 nested gradient, as well as fluorescent pH standards and a DMSO inhibitor mix (all reagents were obtained from ProteinSimple). The automated CIEF-immunoassay was carried out on the Peggy Sue platform (ProteinSimple) as described previously for the NanoPro platform (ProteinSimple, San Jose, CA, USA) [35,36]. Each microcapillary contained a final peptide concentration of 100 ng/ml for peptides ending at position 40 and 50 ng/ml for peptides ending at position 42, corresponding to ~50 and 25 pg peptide per capillary, respectively, based on an internal capillary volume of roughly 0.5  $\mu$ l. Chemiluminescence detection was carried out using peroxidase-labelled anti mouse secondary antibodies (with 4G8, 80C2 and 82E1) or biotinylated anti-rabbit, anti-mouse or antihuman IgG plus peroxidase-conjugated streptavidin (in case of 24311, 18H6 and the humanized biosimilar antibodies Bapineuzumab and Crenezumab).

### Western blot analysis under denaturing conditions

The sensitivity of the antibody 82E1 and the biosimilar Bapineuzumab antibody was further analysed by

urea-bicine/bis-tris/Tris/sulphate sodium dodecyl sulphate (SDS)-PAGE followed by western immunoblotting. Stock solutions of synthetic A $\beta$ <sub>1–40</sub> were prepared in sample buffer (0.36 M bis-tris, 0.16 M bicine, 15% wt/vol sucrose, 1% wt/vol SDS and 0.0075% wt/vol bromophenol blue) and stored at –80°C. Different amounts of A $\beta$ <sub>1–40</sub> peptides (25–100 pg and 25–100 ng respectively) were loaded and separated by urea-bicine/bis-tris/Tris/sulphate SDS-PAGE and analysed by immunoblotting as previously described [40]. The blotting membranes were blocked in 2% enhanced chemiluminescence (ECL) advance blocking agent (GE Healthcare Life Sciences, Little Chalfont, UK) in phosphate-buffered saline (PBS) with 0.075% Tween 20 (PBS-T) for 1 h at room temperature and probed with the primary antibody 82E1 or the biosimilar Bapineuzumab antibody (0.5  $\mu$ g/ $\mu$ l in PBS-T) at 4°C overnight. After three washing steps with PBS-T, biotinylated goat anti-mouse IgG (1:3000 in PBS-T; Life Technologies, Carlsbad, CA, USA) for 82E1 and biotinylated goat anti-human IgG (DAKO, Glostrup, Denmark, 1:3000) for Bapineuzumab, followed by streptavidin-HRP, were employed as secondary reagents. Chemiluminescent signals obtained with ECL Prime Western Blotting Detection Reagent (GE Healthcare Life Sciences) were recorded.

### Human brain samples

Paraffin-embedded human brain samples from sporadic AD ( $n = 20$ ; mean age  $84.45 \pm 6.45$ , average *post mortem* interval (PMI) =  $4:37 \pm 0:56$  h; 14 females, 6 males), nondemented controls (NDC;  $n = 11$ ; mean age  $84.18 \pm 7.17$ , average PMI =  $8:11 \pm 5:54$  h; 7 females, 4 males) and Down syndrome (DS;  $n = 2$ ; mean age  $61.0 \pm 4.24$ , average PMI =  $5:12 \pm 1:21$  h; 1 female, 1 male) were obtained from the Netherlands Brain Bank (Table 1). Samples exclusively from the medial frontal gyrus region of the brain were used in the analysis. This study was approved by the ethical committee of the University Medical Center Göttingen.

### Immunohistochemical staining and semi-quantitative analyses

Immunohistochemistry was performed on 4  $\mu$ m paraffin sections as previously described [41]. In brief, following deparaffinization in xylene and rehydration in a

**Table 1.** Demographic and pathological data of sporadic AD cases, Down syndrome cases and NDC subjects

Case	Age (years)	Gender	ApoE	Braak stage	Amyloid	PMI (h)	CAA
Sporadic AD cases							
AD 1	86	f	3/3	IV	B	04:10	No
AD 2	90	f	4/4	VI	C	04:00	Severe
AD 3	85	f	3/3	VI	C	04:00	Mild
AD 4	88	f	3/3	IV	C	03:30	Mild
AD 5	87	f	4/3	VI	C	06:15	Distinct
AD 6	92	m	3/3	IV	C	03:30	n.d.
AD 7	91	f	3/3	IV	C	03:45	Distinct
AD 8	73	m	4/4	IV	C	05:30	Severe
AD 9	93	f	3/3	IV	C	06:15	No
AD 10	92	f	3/3	IV	C	05:10	n.d.
AD 11	78	m	4/3	V	C	06:00	Distinct
AD 12	82	f	3/3	V	C	04:25	Severe
AD 13	82	f	4/4	V	C	03:05	Distinct
AD 14	77	m	4/3	V	C	04:30	Distinct
AD 15	89	m	3/3	V	C	04:05	No
AD 16	81	m	n.d.	IV	C	04:50	Mild
AD 17	91	f	4/3	IV	B	04:15	Mild
AD 18	79	f	4/3	IV	B/C	05:20	Distinct
AD 19	70	f	3/3	VI	C	05:20	Severe
AD 20	83	f	4/3	VI	C	04:30	Mild
NDC 1	82	f	3/3	I	0	11:30	No
NDC 2	72	f	4/3	II	B	05:30	No
NDC 3	89	f	n.d.	III	0	03:52	No
NDC 4	78	f	3/3	I	A	04:50	No
NDC 5	73	m	3/3	0	0	24:45	No
NDC 6	70	m	3/2	0	0	07:30	n.d.
NDC 7	84	m	3/3	I	0	09:00	No
NDC 8	87	f	n.d.	II	0	05:30	No
NDC 9	93	f	3/3	II	0	05:50	No
NDC 10	87	m	3/3	III	A	06:10	No
NDC 11	90	f	3/3	III	A	06:05	No
DS 1	64	f	3/3	V	C	04:15	Distinct
DS 2	58	m	4/3	VI	n.d.	06:10	Distinct

ApoE, apolipoprotein E; AD, Alzheimer's disease; NDC, nondemented control subject; DS, Down syndrome; PMI, *post mortem* interval; n.d., not determined; CAA, cerebral amyloid angiopathy.

descending series of ethanol (100%, 95%, 70%), endogenous peroxidases were blocked by incubation in 0.3% H<sub>2</sub>O<sub>2</sub> in PBS for 30 min. Sections were boiled in 0.01 M citrate buffer and incubated in 88% formic acid for antigen retrieval. Prior to the incubation with the primary antibodies, nonspecific-binding sites were blocked by treatment with 4% skim milk in PBS containing 10% foetal calf serum for 1 h at room temperature. The following antibodies were used for the detection of different A $\beta$  variants: 80C2 (mouse mAb, Synaptic Systems, 2  $\mu$ g/ml) and 82E1 (mouse mAb, IBL International, Hamburg, Germany, 1  $\mu$ g/ml) for the detection of A $\beta$ <sub>1–x</sub>; D3E10 (rabbit mAb, Cell Signaling Technology, Danvers, MA, USA, 1:1000) against A $\beta$ <sub>42</sub>; 24311 (rabbit pAb [37], 1:500) against the N-terminus of A $\beta$ ; 18H6 (mouse

mAb, 1.9  $\mu$ g/ml [20]) and 029-2 (guinea-pig pAb [36], 2.36  $\mu$ g/ml) for the detection of A $\beta$  starting with Phe at position 4; and pAb77 (rabbit pAb [40], 2.32  $\mu$ g/ml) against A $\beta$ <sub>2–x</sub>. Lastly, the humanized biosimilar Bapineuzumab ([38,42], 0.7  $\mu$ g/ml) and Crenezumab ([38,42]; 0.85  $\mu$ g/ml) antibodies were used in this study. Biotinylated secondary anti-guinea pig (Dianova, Hamburg, Germany), anti-mouse, anti-rabbit and anti-human antibodies (all DAKO) were used in a 1:200 dilution. Staining was visualized using the ABC method, with a Vectastain kit (Vector Laboratories, Burlingame, CA, USA) and diaminobenzidine as chromogen. Counterstaining was carried out with haematoxylin. In order to perform a semi-quantitative analysis of the staining, the sections were evaluated in a blinded fashion using a

BX51 microscope (Olympus, Hamburg, Germany) equipped with a Moticam Pro 282 camera (Motic, Wetzlar, Germany). The following semi-quantitative scoring criteria were used to assess parenchymal and vascular staining: 0 = no staining, 0.5 = barely detectable staining, 1 = weak staining, 2 = moderate staining, 3 = extensive staining. Heat maps were plotted using GraphPad Prism 8.3.0 (GraphPad, San Diego, CA, USA).

## Results

### Determination of antibody selectivity using CIEF-immunoassays

In the present report, a comparative analysis of the immunohistochemical staining profile of antibodies detecting either full-length or N-terminally truncated A $\beta$  species was carried out. First, we studied the selectivity of the different antibodies using the CIEF immunoassay employing a variety of synthetic N-terminal truncated A $\beta$  peptide variants. Antibody 4G8, directed against a central epitope (17–24) which is present in all peptides utilized in the current analysis, was used as a control antibody. As expected, 4G8 detected the entire set of A $\beta$  peptides (A $\beta_{3-40}$ , A $\beta_{1-40}$ , A $\beta_{2-40}$ , A $\beta_{3-40}$ , A $\beta_{pE3-40}$ , A $\beta_{4-40}$ , A $\beta_{5-40}$ , A $\beta_{11-40}$ ) (Figure S1). Next, antibodies presumed to detect selectively either full-length A $\beta$  species starting with Asp-1 or N-terminally truncated species, such as A $\beta_{4-x}$  starting with a phenylalanine residue at position 4, were analysed. The mouse monoclonal antibodies 82E1 and 80C2 detected the N-terminus of A $\beta$  and produced a clear signal for A $\beta_{1-40}$  without appreciable cross-reactivity with either the N-terminally elongated peptide variant A $\beta_{3-40}$  or the N-terminally truncated species such as A $\beta_{2-40}$ , A $\beta_{3-40}$  or A $\beta_{4-40}$  under the tested conditions. Thus, it appears that these two particular antibodies require a free N-terminal aspartic acid residue in position 1 of the A $\beta$  sequence (Asp-1) (Figure 1). In contrast, the mouse monoclonal antibody 18H6 showed a clear signal only with synthetic A $\beta$  peptides starting with the Phe residue (A $\beta_{4-x}$ ), without any noticeably cross-reactivity with longer or shorter A $\beta$  peptides tested, thereby confirming its high selectivity for A $\beta_{4-x}$  variants (Figure 1). The polyclonal antibody 24311 showed a profile comparable to 4G8, except for the fact that it did not detect elongated A $\beta_{3-40}$  peptides and only weakly reacted with full-length A $\beta_{1-40}$  (Figure 1).

Finally, the N-terminal selectivity of the recombinant biosimilar human antibodies Bapineuzumab and Crenezumab was determined. While Bapineuzumab only detected the full-length A $\beta_{1-40}$  peptides without showing signals for either elongated (A $\beta_{3-40}$ ) or any of the N-terminally truncated A $\beta$  variants (Figure 1), Crenezumab detected the entire range of A $\beta$  peptides employed (Figure 1), resembling the peptide pattern detected by the pan-specific control antibody 4G8 (Figures S1 and S2). As A $\beta$  species ending at 42 could have a very distinct conformation that might eventually alter immunoreactivity towards epitopes even located at the N-terminus, we additionally tested the detection of selected A $\beta_{42}$  variants with antibodies 4G8, 80C2, 18H6 and the biosimilar antibodies Bapineuzumab and Crenezumab. In qualitative terms, the tested antibodies showed the same detection profile as with the A $\beta_{40}$  variants (Figures S2 and S3).

### Comparative A $\beta$ staining profiles in human sporadic AD, NDC and DS cases

Most of the sporadic AD cases, as well as the two DS samples, demonstrated high abundance of both extracellular amyloid plaques and vascular deposits detected by the pan-A $\beta$  antibody 24311 (Figures 2A and 3A), as well as the A $\beta_{42}$ -selective antibody D3E10 (Figures 2B and 5). In contrast, antibodies 82E1 (Figure 2C) and 80C2 (Figures 2D and 4B), selectively recognizing Asp-1, showed a much weaker staining of extracellular plaques, but intensely stained cerebrovascular amyloid deposits (Figure 3B,C). In general, 82E1 detected a more widespread pattern of extracellular deposits, while the staining profile of both antibodies largely overlapped with regard to parenchymal or meningeal vascular amyloid accumulation. The polyclonal antibody Ab77, directed against A $\beta_{2-x}$  starting with an alanine residue, detected only few plaques in most of the AD cases (Figures 2E and 5). In contrast, A $\beta_{2-x}$ -positive plaques were found in substantial amounts in both DS cases, as well as in meningeal and parenchymal vessels in the majority of AD cases (Figure 5).

Both antibodies capable of recognizing the free Phe residue at position 4 (029-2 and 18H6) showed abundant amyloid plaque immunoreactivity in the brain parenchyma of individuals suffering from sporadic AD (Figure 2F) and detected vascular deposits in approximately half of the AD cases (Figure 5). Finally, the two

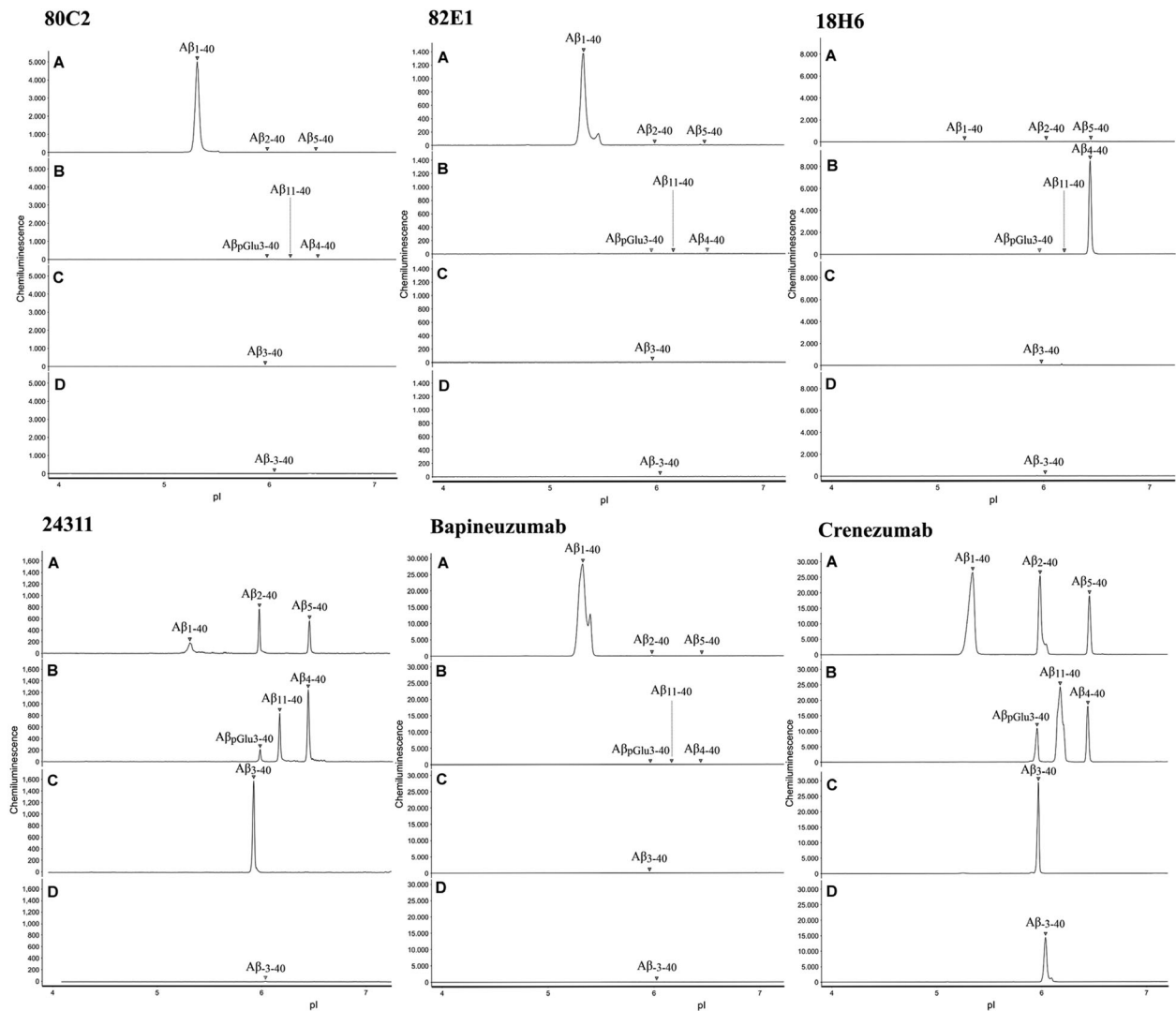


**Figure 1.** Assessment of antibody selectivity by capillary isoelectric focusing immunoassay. Synthetic amyloid- $\beta$  (A $\beta$ ) peptides with different N-termini were separated by isoelectric focusing in microcapillaries, immobilized by a photochemical reaction and probed with the indicated primary antibodies. Chemiluminescence detection was achieved with peroxidase-labelled anti mouse antibodies (80C2, 82E1). In case of 24311, 18H6 and the humanized biosimilar antibodies Bapineuzumab and Crenezumab, biotinylated anti-rabbit, anti-mouse or anti-human IgG plus peroxidase-conjugated streptavidin were employed. For each one of the indicated primary antibodies, a mixture of A $\beta$ <sub>1-40</sub>, A $\beta$ <sub>2-40</sub> and A $\beta$ <sub>5-40</sub> (electropherogram A), a mixture of A $\beta$ <sub>pGlu3-40</sub>, A $\beta$ <sub>4-40</sub> and A $\beta$ <sub>11-40</sub> (B), A $\beta$ <sub>3-40</sub> (C) and N-terminally elongated A $\beta$ <sub>-3-40</sub> (APP669-711) (D) were assessed. To facilitate the evaluation of the selectivity for specific N-terminal A $\beta$  variants, the electropherograms were scaled for each primary antibody according to the maximum signal that was observed. Note that the signals obtained with the humanized biosimilar antibodies Bapineuzumab and Crenezumab were substantially higher than with the mouse monoclonals. Presumably, in these two cases the combination of a biotinylated anti human antibody and peroxidase-conjugated streptavidin provided highly efficient signal amplification.

biosimilar recombinant antibodies Crenezumab and Bapineuzumab were analysed. While Crenezumab demonstrated considerable immunoreactivity and showed a weak to moderate staining pattern in the majority of sporadic AD patients analysed (Figures 2G and 5), Bapineuzumab detected extracellular plaques in all AD and DS cases with mainly moderate to high

intensity (Figures 2H and 5). Both antibodies showed a largely concordant staining profile with regard to parenchymal and meningeal vascular deposits in AD cases with intense immunoreactivity in the DS cases (Figure 5; Figure S4).

In the control cases considered here, the overall immunoreactivity was predominantly negative, with



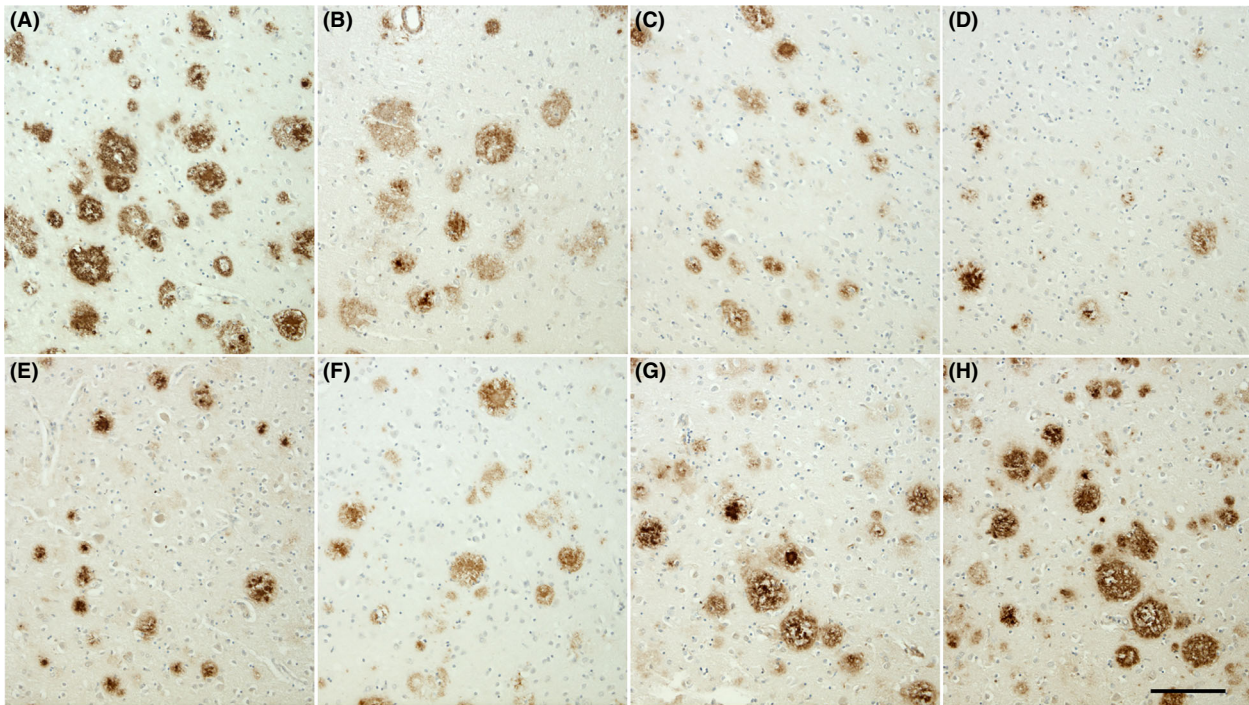


**Figure 2.** Immunohistochemical staining of extracellular amyloid- $\beta$  (A $\beta$ ) peptides in a sporadic Alzheimer's disease (AD) case (AD case 20). Parallel sections of the frontal cortex of a sporadic AD case were stained with the pan-A $\beta$  antibody 24311 (A), the A $\beta$ <sub>42</sub>-specific antibody D3E10 (B), the A $\beta$ <sub>1-x</sub>-specific antibodies 82E1 (C) and 80C2 (D), the A $\beta$ <sub>2-x</sub>-specific antibody A $\beta$  77 (E), the A $\beta$ <sub>4-x</sub>-specific antibody 18H6 (F), as well as the biosimilar human antibodies Crenezumab (G) and Bapineuzumab (H). Scale bar: A–H = 100  $\mu$ m. [Colour figure can be viewed at [wileyonlinelibrary.com](http://wileyonlinelibrary.com)]

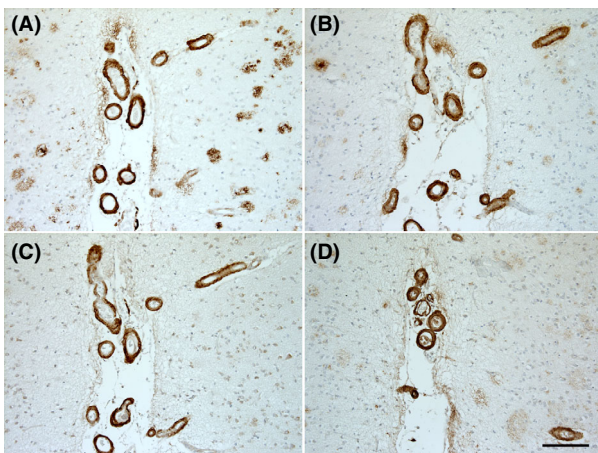


**Figure 3.** A $\beta$ -immunoreactivity of parenchymal vessels in a sporadic Alzheimer's disease (AD) case (AD case 5). Parallel sections of the frontal cortex of a sporadic AD case were stained with the pan-A $\beta$  antibody 24311 (A), the A $\beta$ <sub>1-x</sub>-specific antibodies 82E1 (B) and 80C2 (C), as well as the biosimilar human antibody Bapineuzumab (D). Scale bar: A–D = 100  $\mu$ m. [Colour figure can be viewed at [wileyonlinelibrary.com](http://wileyonlinelibrary.com)]

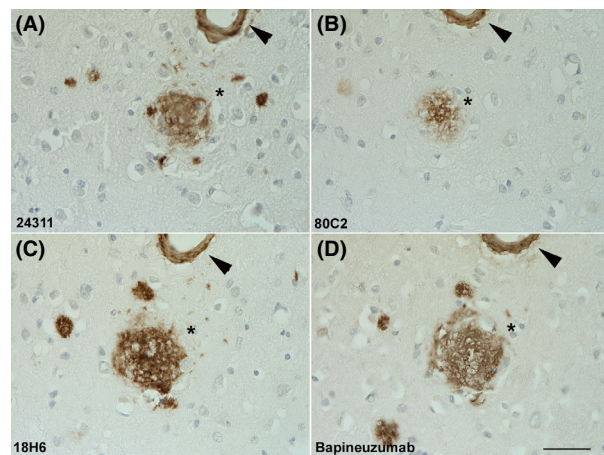


**Figure 4.** High magnification images of 24311 (A), 80C2 (B), 18H6 (C) and Bapineuzumab (D) antibodies in adjacent sections (Alzheimer's disease case 18). While immunoreactivity of all antibodies is comparable in parenchymal vessels (arrowhead), 80C2 shows considerably less staining in parenchymal extracellular deposits compared to the other antibodies (\*). Scale bar: A–D = 33  $\mu$ m. [Colour figure can be viewed at [wileyonlinelibrary.com](http://wileyonlinelibrary.com)]

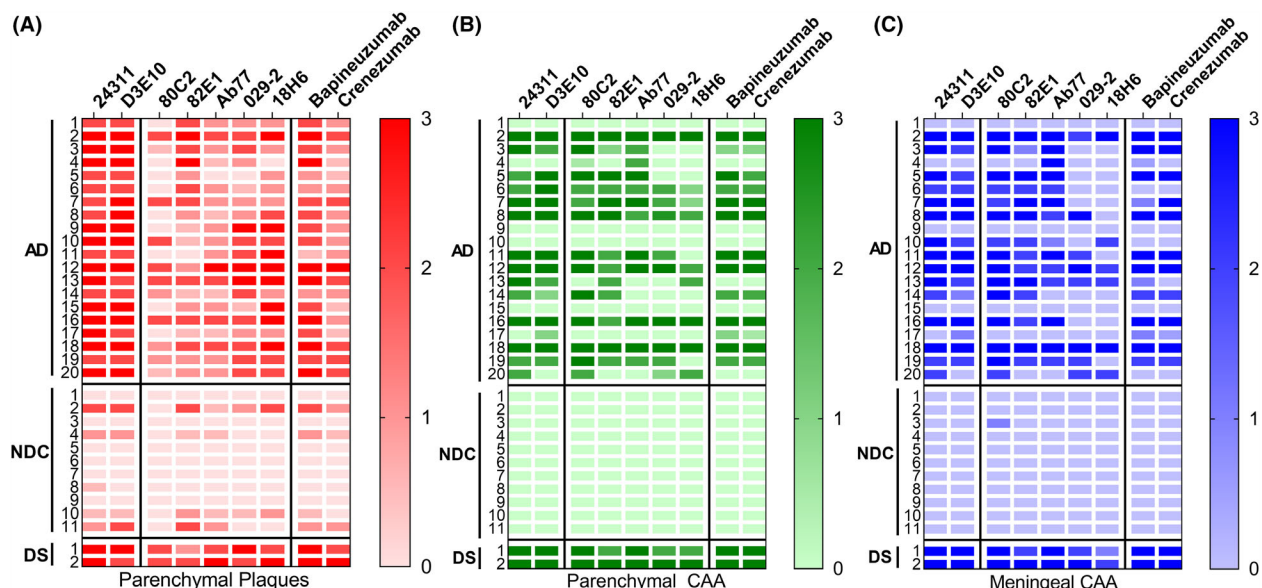


**Figure 5.** Semiquantitative analyses of the immunostaining. Heat maps illustrating the results of the immunostaining of parenchymal plaques (A), parenchymal (B) and meningeal CAA (C). AD, sporadic Alzheimer's disease; NDC, nondemented control; DS, Down's syndrome; CAA, cerebral amyloid angiopathy. [Colour figure can be viewed at [wileyonlinelibrary.com](http://wileyonlinelibrary.com)]

four out of 11 cases displaying a weak to moderate extracellular amyloid plaques staining with the pan-A $\beta$  antibody 24311 and A $\beta_{42}$  antibody D3E10. The control cases were largely negative with the antibodies recognizing N-terminal truncated A $\beta$  variants and parenchymal and meningeal vascular deposits were absent with all the analysed antibodies (Figure 5; Figures S5 and S6).

A comparative analysis of 24311 (pan-Ab), 80C2 (A $\beta_{1-x}$ ), 18H6 (A $\beta_{4-x}$ ) and Bapineuzumab underscored the above-mentioned differences in immunoreactivity with regard to full-length A $\beta$  peptides. While 24311, 18H6 and Bapineuzumab detected the identical extracellular A $\beta$  deposit in parallel sections with comparable sensitivity; the signal generated by 80C2 was strongly reduced (Figure 4, asterisk). Interestingly, all four antibodies showed a comparable staining intensity of parenchymal vessels (Figure 4, arrowhead), corroborating the quantification of parenchymal CAA (Figure 5).

#### Evidence of a conformational preference of the biosimilar antibody Bapineuzumab

In the immunohistochemical analysis, the biosimilar antibody Bapineuzumab detected substantially more extracellular amyloid deposits than the other A $\beta_{1-x}$ -

specific antibodies 80C2 and 82E1. Thus, it appears that under the experimental conditions employed (i.e. formalin fixation and pretreatment with formic acid for sensitization), Bapineuzumab is more sensitive than the other A $\beta_{1-x}$ -specific antibodies tested. To assess whether in addition to the amino acid sequence (primary structure), the conformation of the A $\beta$  peptides may impact the strength of the recognition by the different antibodies, we compared Bapineuzumab and 82E1 by urea-bicaine/bis-tris/Tris/sulphate SDS-PAGE followed by Western blotting. Different amounts of A $\beta_{1-40}$  peptides (25–100 pg and 25–100 ng respectively) were separated on SDS gels containing 8 M urea, blotted onto PVDF membranes and probed with either Bapineuzumab or 82E1 antibodies. While no appreciable signals were observed with amounts up to 100 pg A $\beta_{1-40}$  with Bapineuzumab (Figure 6A), even minute amounts as low as 25 pg of A $\beta_{1-40}$  were clearly detected with 82E1 (Figure 6B). The comparatively much higher detection sensitivity of 82E1 in the urea Western blot assays suggests a strong impact of the A $\beta$  peptide conformation on its binding by Bapineuzumab. While in immunohistochemistry (i.e. without preanalytical A $\beta$  denaturation with SDS and Urea), Bapineuzumab displayed very high detection sensitivity, it appeared to be substantially less sensitive on Urea-SDS-PAGE-Western blots.



## Discussion

The presence of A $\beta_{40}$  and A $\beta_{42}$  peptides has been extensively evaluated in human brain. Due to the commercial availability of A $\beta$  end-specific antibodies, a multitude of neuropathological and biochemical studies dealing with the role of these peptides during ageing and the course of AD have been published in recent years. In addition to full-length A $\beta$  starting with Asp-1 (e.g. A $\beta_{1-40}$ , A $\beta_{1-42}$ ), a variety of N- and C-terminally truncated A $\beta$  peptides can be detected in human brain samples [14,15,43-45]. Mass spectrometry allows for the unequivocal identification of A $\beta$  variants present in brain amyloid but provides only limited information in terms of spatial localization or distribution of specific A $\beta$  species. On the other hand, the use of A $\beta$  antibodies in applications such as immunohistochemistry is largely dependent on the careful characterization of antibody selectivity and sensitivity. We therefore set out to determine the specificity of a variety of commonly used A $\beta$  antibodies using CIEFs, by employing a wide range of N-terminally elongated (A $\beta_{-3-40}$ ), full-length (A $\beta_{1-40}$ ), as well as N-terminally truncated (A $\beta_{2-40}$ , A $\beta_{3-40}$ , A $\beta_{pE3-40}$ , A $\beta_{4-40}$ , A $\beta_{5-40}$ , A $\beta_{11-40}$ ) A $\beta$  peptide variants. The widely used 4G8 antibody, recognizing a central epitope within the A $\beta$  sequence, detected all A $\beta$  species employed as anticipated and served as a control

antibody. We further confirmed the high selectivity of 80C2 [46] and 18H6 [20], for A $\beta_{1-x}$  and A $\beta_{4-x}$  respectively.

The immunohistochemical analysis employing this entire set of antibodies against full-length, N-truncated, the A $\beta$  C-terminus (A $\beta_{42}$ ) or total A $\beta$  revealed the expected heterogeneity. While both 80C2 and 82E1 (detecting Asp-1) on the one hand, or 029-2 [36] and 18H6 (detecting Phe-4) on the other showed an exactly concordant profile in terms of selectivity in the CIEF assays, the staining patterns with regard to extracellular amyloid plaque as well as vascular deposition revealed some distinctions. 82E1 showed a more widespread pattern of extracellular deposits compared to 80C2, disclosing a pattern associable to a classical neuritic plaque staining. While 029-2 and 18H6 intensely stained amyloid plaque cores, the latter appeared to present a more abundant pattern in the cases employed in this study. This might be attributed to differences in antibody detection sensitivities, as well as an additional impact of A $\beta$  peptide conformation beyond sequence specificity. As expected, sporadic AD cases showed a more intense staining pattern than the employed NDC cases in general. The substantial immunoreactivity of NDC case 2 with several antibodies can be attributed to the presence of medium densities of amyloid deposits (amyloid stage B, see Table 1).

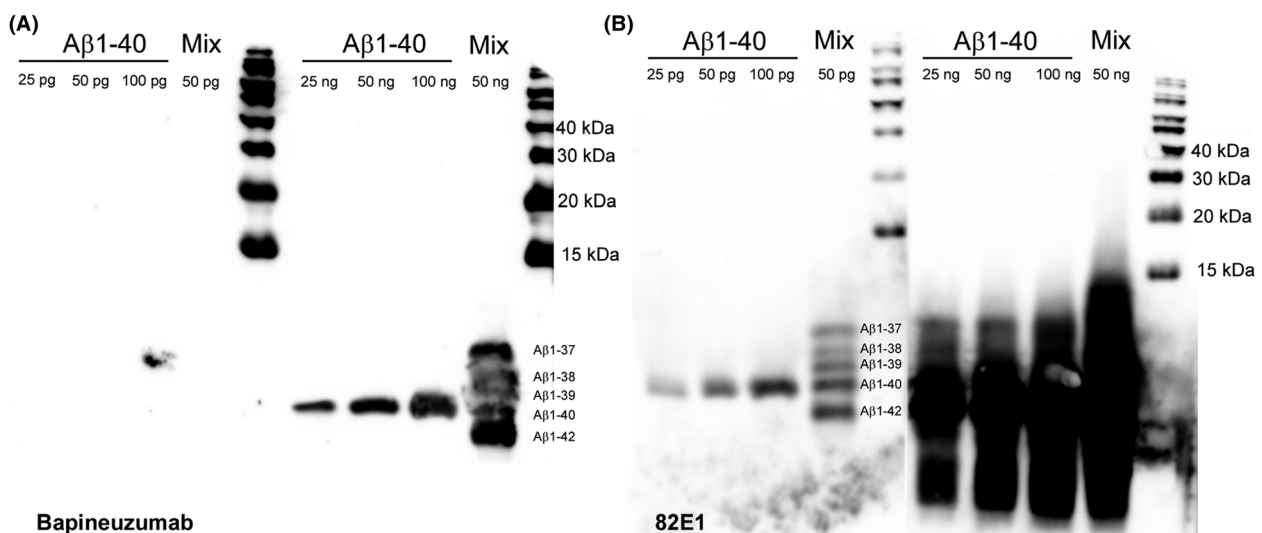


**Figure 6.** Differential sensitivity of N-terminal-specific antibodies Bapineuzumab and 82E1 under denaturing conditions. Under denaturing conditions in the SDS-PAGE, Bapineuzumab (A) shows a roughly 1000-fold lower sensitivity compared to 82E1 (B), which is capable of detecting A $\beta_{1-40}$  peptides in amounts as low as 25 pg.

The PMI is a variable parameter in neuropathological analyses that might influence protein and nucleic acid integrity. In this study, the average PMI of the AD samples (<5 h) and control samples (<9 h) were relatively short, which might have only a limited impact on protein denaturation. It has been shown by others that a PMI of over 50 h did not change the immune staining profiles of several proteins [47], and no correlation was found between PMI and the relative abundance of most of the N-truncated variants analysed here [18].

Despite several setbacks [7–13], passive immunization with anti-amyloid monoclonal antibodies is still debated as a potential disease-modifying therapy, and clinical trials are ongoing [48]. We analysed the biosimilar Bapineuzumab and Crenezumab antibodies, which both had been evaluated in clinical trials and did not meet their primary endpoints [8,49,50]. While Crenezumab, similar to the pan-specific anti A $\beta$  monoclonal 4G8, detected the whole set of A $\beta$  variants tested, Bapineuzumab selectively detected A $\beta_{1-40}$  starting with Asp and did not detect N-terminally elongated or truncated A $\beta$  species. Crenezumab has been described as a fully humanized immunoglobulin isotype G4 (IgG4) monoclonal antibody that binds to A $\beta$  oligomers with high affinity, while also maintaining the ability to bind to other forms of A $\beta$  [51]. Atomic structures show that Crenezumab and the clinical antibody Solanezumab bind A $\beta$  peptides in a virtually identical conformation of consecutive residues in the central epitope ( $\sim$ A $\beta_{13-24}$ ) [52,53], containing the A $\beta$  aggregation nucleation site KLVFFA. This is consistent with our results from the CIEF assay, where Crenezumab behaved in the same way as the widely used 4G8 antibody (epitope A $\beta_{17-21/23}$ ) [54,55] and the findings of Watt and colleagues in *ex vivo* SELDI-TOF experiments in AD-affected tissue [36].

The observed selectivity of Bapineuzumab for the free N-terminal Asp residue confirms and extends earlier studies. Surface plasmon resonance binding response curves resulted in essentially identical  $k_d$  values of Bapineuzumab for different peptides starting with Asp-1, such as A $\beta_{1-28}$ , A $\beta_{1-40}$  and A $\beta_{1-42}$ . No binding was detected between the antibody and A $\beta$  species with an altered N-terminus [38]. Analysis of the crystal structure of the humanized antigen-binding fragment in complex with A $\beta_{1-28}$  revealed that the free N-terminus was critical for A $\beta$  binding. This structure analysis

suggests that Bapineuzumab recognizes the N-terminal end of A $\beta$  in a helical conformation that is stabilized by five putative intramolecular hydrogen bonds [53]. The experiments performed in this study support these assumptions, showing in addition that neither elongated (A $\beta_{-3-40}$ ) or peptides starting with an N-terminal alanine residue (A $\beta_{2-40}$ ) are recognized. With regard to the immunohistochemical staining of parenchymal plaques, Bapineuzumab seems to stain a higher proportion of extracellular deposits than 80C2 or 82E1, which are also directed against the free N-terminal Asp residue present in full-length A $\beta$  peptides. Under the strongly denaturing conditions employed in the Urea-SDS PAGE/ Western blot analysis, the opposite was observed with 82E1 detecting A $\beta_{1-40}$  peptides at  $\sim$ 1000-fold lower concentrations than Bapineuzumab. We conclude that, the helical conformation of the A $\beta$  - N-terminus recognized by Bapineuzumab [53] is probably essentially destroyed by heating the samples in the presence of SDS prior to electrophoresis, but not by formalin fixation and formic acid treatment used in immunohistochemistry. Thus, Bapineuzumab, but not 82E1, appears to be particularly sensitive to specific conformational properties of A $\beta$ .

The conformational preference of antibodies may play a critical role both at a clinical level, when employed in, for example immunotherapy, as well as when they are utilized as research tools in preclinical settings. This adds to the complexity determined by the heterogeneous composition of plaques and the differences in spatial localization or distribution of specific A $\beta$  species and impedes approaches to unravel disease mechanisms and find potentially suitable targets in AD.

## Acknowledgement

The generous gift of A $\beta_{-3-40/42}$  peptides from Dr H.-J. Knölker, Dresden and the expert technical assistance of Petra Rieper is gratefully acknowledged.

## Funding

Financial support of the Alzheimer Forschung Initiative (grant 16013 to O.W.), Alzheimer Stiftung Göttingen (to O.W.), Gerhard-Hunsmann Stiftung (to O.W.) and National Institutes of Health (NIH AG059695 to J.G.) is gratefully acknowledged. JW is supported by an IlídioPinho professorship; iBiMED (UID/BIM/04501/

2020) and FCT project PTDC/DTP-PIC/5587/2014, at the University of Aveiro, Portugal.

## Author contributions

SZ performed experiments and together with HWK analysed data and contributed to the manuscript draft. KS performed experiments and JG, AR, LAM, TAB and JW provided reagents and contributed to the interpretation of findings and revision of the manuscript. OW designed the study, analysed data and wrote the manuscript. All authors read and approved the final manuscript.

## Conflict of interest

The authors declare that they have no competing interests.

## Ethical approval and consent to participate

All procedures involving human tissue have been approved by the ethical committee of the University Medical Center, Göttingen (Protocol number 12/1/15). All tissues have been received from the Netherlands Brain Bank (NBB) and all material and data collected by the NBB are obtained on the basis of written informed consent.

## Data availability statement

The data that support the findings of this study are available from the corresponding author upon reasonable request.

## References

- 1 Nhan HS, Chiang K, Koo EH. The multifaceted nature of amyloid precursor protein and its proteolytic fragments: friends and foes. *Acta Neuropathol* 2015; **129**: 1–19
- 2 Hardy J, Allsop D. Amyloid deposition as the central event in the aetiology of Alzheimer's disease. *Trends Pharmacol Sci* 1991; **12**: 383–8
- 3 Bertram L, Lill CM, Tanzi RE. The genetics of Alzheimer disease: back to the future. *Neuron* 2010; **68**: 270–81
- 4 Weggen S, Behr D. Molecular consequences of amyloid precursor protein and presenilin mutations causing autosomal-dominant Alzheimer's disease. *Alzheimers Res Ther* 2012; **4**: 9
- 5 Arriagada PV, Growdon JH, Hedley-Whyte ET, Hyman BT. Neurofibrillary tangles but not senile plaques parallel duration and severity of Alzheimer's disease. *Neurology* 1992; **42**: 631–9
- 6 Lyons B, Kwan AH, Truscott RJW. Spontaneous cleavage of proteins at serine and threonine is facilitated by zinc. *Aging Cell* 2016; **15**: 237–44
- 7 Doody RS, Thomas RG, Farlow M, Iwatsubo T, Vellas B, Joffe S, et al. Phase 3 trials of Solanezumab for mild-to-moderate Alzheimer's disease. *New Engl J Med* 2014; **370**: 311–21
- 8 Salloway S, Sperling R, Fox NC, Blennow K, Klunk W, Raskind M, et al. Two phase 3 trials of Bapineuzumab in mild-to-moderate Alzheimer's disease. *New Engl J Med* 2014; **370**: 322–33
- 9 Cummings JL, Cohen S, van Dyck CH, Brody M, Curtis C, Cho W, et al. ABBY – a phase 2 randomized trial of Crenezumab in mild to moderate Alzheimer disease. *Neurology* 2018; **90**: e1889–97
- 10 Ostrowitzki S, Lasser RA, Dorflinger E, Scheltens P, Barkhof F, Nikolcheva T, et al. A phase III randomized trial of gantenerumab in prodromal Alzheimer's disease. *Alzheimers Res Ther* 2017; **9**: 95
- 11 Selkoe DJ. Alzheimer disease and aducanumab: adjusting our approach. *Nat Rev Neurol* 2019; **15**: 365–6
- 12 Landen JW, Cohen S, Billing CB, Cronenberger C, Styren S, Burstein AH, et al. Multiple-dose ponesumab for mild-to-moderate Alzheimer's disease: Safety and efficacy. *Alzheimer's Dement: Transl Res Clin Intervent* 2017; **3**: 339–47
- 13 Honig LS, Vellas B, Woodward M, Boada M, Bullock R, Borrie M, et al. Trial of Solanezumab for mild dementia due to Alzheimer's disease. *New Engl J Med* 2018; **378**: 321–30
- 14 Portelius E, Bogdanovic N, Gustavsson MK, Volkman I, Brinkmalm G, Zetterberg H, et al. Mass spectrometric characterization of brain amyloid beta isoform signatures in familial and sporadic Alzheimer's disease. *Acta Neuropathol* 2010; **120**: 185–93
- 15 Moore BD, Chakrabarty P, Levites Y, Kukar TL, Baine AM, Moroni T, et al. Overlapping profiles of abeta peptides in the Alzheimer's disease and pathological aging brains. *Alzheimers Res Ther* 2012; **4**: 18
- 16 Gkanatsiou E, Portelius E, Toomey CE, Blennow K, Zetterberg H, Lashley T, et al. A distinct brain beta amyloid signature in cerebral amyloid angiopathy compared to Alzheimer's disease. *Neurosci Lett* 2019; **701**: 125–31
- 17 Rostagno A, Neubert TA, Ghiso J. Unveiling brain A $\beta$  heterogeneity through targeted proteomic analysis. *Methods Mol Biol* 2018; **1779**: 23–43
- 18 Wildburger NC, Esparza TJ, LeDuc RD, Fellers RT, Thomas PM, Cairns NJ, et al. Diversity of amyloid-beta

- proteoforms in the alzheimer's disease brain. *Sci Rep* 2017; **7**: 9520
- 19 Tomidokoro Y, Rostagno A, Neubert TA, Lu Y, Rebeck GW, Frangione B, et al. Iowa variant of familial Alzheimer's disease: accumulation of posttranslationally modified A $\beta$ D23N in parenchymal and cerebrovascular amyloid deposits. *Am J Pathol* 2010; **176**: 1841–54
  - 20 Cabrera E, Mathews P, Mezhericher E, Beach TG, Deng J, Neubert TA, et al. A $\beta$  truncated species: Implications for brain clearance mechanisms and amyloid plaque deposition. *Biochim Biophys Acta* 2018; **1864**: 208–25
  - 21 He W, Barrow CJ. The A beta 3-pyroglutamyl and 11-pyroglutamyl peptides found in senile plaque have greater beta-sheet forming and aggregation propensities in vitro than full-length A beta. *Biochemistry* 1999; **38**: 10871–7
  - 22 Saido TC, Iwatsubo T, Mann DM, Shimada H, Ihara Y, Kawashima S. Dominant and differential deposition of distinct beta-amyloid peptide species, A beta N3(pE), in senile plaques. *Neuron* 1995; **14**: 457–66
  - 23 Kumar S, Rezaei-Ghaleh N, Terwel D, Thal DR, Richard M, Hoch M, et al. Extracellular phosphorylation of the amyloid beta-peptide promotes formation of toxic aggregates during the pathogenesis of Alzheimer's disease. *EMBO J* 2011; **30**: 2255–65
  - 24 Kumar S, Wirths O, Stuber K, Wunderlich P, Koch P, Theil S, et al. Phosphorylation of the amyloid beta-peptide at Ser26 stabilizes oligomeric assembly and increases neurotoxicity. *Acta Neuropathol* 2016; **131**: 525–37
  - 25 Pike CJ, Overman MJ, Cotman CW. Amino-terminal deletions enhance aggregation of beta-amyloid peptides in vitro. *J Biol Chem* 1995; **270**: 23895–8
  - 26 Miller DL, Papayannopoulos IA, Styles J, Bobin SA, Lin YY, Biemann K, et al. Peptide compositions of the cerebrovascular and senile plaque core amyloid deposits of Alzheimer's disease. *Arch Biochem Biophys* 1993; **301**: 41–52
  - 27 Lewis H, Beher D, Cookson N, Oakley A, Piggott M, Morris CM, et al. Quantification of Alzheimer pathology in ageing and dementia: age-related accumulation of amyloid-beta(42) peptide in vascular dementia. *Neuropathol Appl Neurobiol* 2006; **32**: 103–18
  - 28 Masters CL, Simms G, Weinman NA, Multhaup G, McDonald BL, Beyreuther K. Amyloid plaque core protein in Alzheimer disease and Down syndrome. *Proc Natl Acad Sci U S A* 1985; **82**: 4245–9
  - 29 Haass C, Selkoe DJ. Soluble protein oligomers in neurodegeneration: lessons from the Alzheimer's amyloid [beta]-peptide. *Nat Rev Mol Cell Biol* 2007; **8**: 101–12
  - 30 Brody DL, Jiang H, Wildburger N, Esparza TJ. Non-canonical soluble amyloid-beta aggregates and plaque buffering: controversies and future directions for target discovery in Alzheimer's disease. *Alzheimer's Res Ther* 2017; **9**: 62
  - 31 Levites Y, Das P, Price RW, Rochette MJ, Kostura LA, McGowan EM, et al. Anti-A $\beta$ 42- and anti-A $\beta$ 40-specific mAbs attenuate amyloid deposition in an Alzheimer disease mouse model. *J Clin Invest* 2006; **116**: 193–201
  - 32 Wilcock DM, Alamed J, Gottschall PE, Grimm J, Rosenthal A, Pons J, et al. Deglycosylated anti-amyloid-beta antibodies eliminate cognitive deficits and reduce parenchymal amyloid with minimal vascular consequences in aged amyloid precursor protein transgenic mice. *J Neurosci* 2006; **26**: 5340–6
  - 33 Pfeifer M, Boncristiano S, Bondolfi L, Stalder A, Deller T, Staufenbiel M, et al. Cerebral hemorrhage after passive anti-A $\beta$  immunotherapy. *Science* 2002; **298**: 1379
  - 34 Wilcock DM, Rojiani A, Rosenthal A, Subbarao S, Freeman MJ, Gordon MN, et al. Passive immunotherapy against Abeta in aged APP-transgenic mice reverses cognitive deficits and depletes parenchymal amyloid deposits in spite of increased vascular amyloid and microhemorrhage. *J Neuroinflammation* 2004; **1**: 24
  - 35 Haußmann U, Jahn O, Linning P, Janßen C, Liepold T, Portelius E, et al. Analysis of amino-terminal variants of amyloid- $\beta$  peptides by capillary isoelectric focusing immunoassay. *Anal Chem* 2013; **85**: 8142–9
  - 36 Wirths O, Walter S, Kraus I, Klafki HW, Stazi M, Oberstein TJ, et al. N-truncated A $\beta$ 4–x peptides in sporadic Alzheimer's disease cases and transgenic Alzheimer mouse models. *Alzheimers Res Ther* 2017; **9**: 80
  - 37 Saul A, Sprenger F, Bayer TA, Wirths O. Accelerated tau pathology with synaptic and neuronal loss in a novel triple transgenic mouse model of Alzheimer's disease. *Neurobiol Aging* 2013; **34**: 2564–73
  - 38 Watt AD, Crespi GA, Down RA, Ascher DB, Gunn A, Perez KA, et al. Do current therapeutic anti-Abeta antibodies for Alzheimer's disease engage the target? *Acta Neuropathol* 2014; **127**: 803–10
  - 39 Beyer I, Rezaei-Ghaleh N, Klafki HW, Jahn O, Haußmann U, Wiltfang J, et al. Solid-phase synthesis and characterization of N-terminally elongated A $\beta$  (–3–x)-peptides. *Chemistry* 2016; **22**: 8685–93
  - 40 Savastano A, Klafki H, Hausmann U, Oberstein TJ, Muller P, Wirths O, et al. N-truncated Abeta 2-X starting with position two in sporadic Alzheimer's disease cases and two Alzheimer mouse models. *J Alzheimers Dis* 2016; **49**: 101–10
  - 41 Wirths O, Multhaup G, Czech C, Feldmann N, Blanchard V, Tremp G, et al. Intraneuronal APP/A beta trafficking and plaque formation in beta-amyloid precursor protein and presenilin-1 transgenic mice. *Brain Pathol* 2002; **12**: 275–86
  - 42 Bouter Y, Noguerola JS, Tucholla P, Crespi GA, Parker MW, Wiltfang J, et al. Abeta targets of the biosimilar antibodies of Bapineuzumab, Crenezumab, Solanezumab in comparison to an antibody against N-

- truncated Abeta in sporadic Alzheimer disease cases and mouse models. *Acta Neuropathol* 2015; **130**: 713–29
- 43 Bayer TA, Wirths O. Focusing the amyloid cascade hypothesis on N-truncated Abeta peptides as drug targets against Alzheimer's disease. *Acta Neuropathol* 2014; **127**: 787–801
- 44 Kummer MP, Heneka MT. Truncated and modified amyloid-beta species. *Alzheimers Res Ther* 2014; **6**: 28
- 45 Wirths O, Zampar S. Emerging roles of N- and C-terminally truncated A $\beta$  species in Alzheimer's disease. *Expert Opin Ther Targets* 2019; **23**: 991–1004
- 46 Walter S, Jumpertz T, Hüttenrauch M, Ogorek I, Gerber H, Storck SE, Zampar S, et al. The metalloprotease ADAMTS4 generates N-truncated A $\beta$ <sub>4-x</sub> species and marks oligodendrocytes as a source of amyloidogenic peptides in Alzheimer's disease. *Acta Neuropathol* 2019; **137**: 239–57
- 47 Blair JA, Wang C, Hernandez D, Siedlak SL, Rodgers MS, Achar RK, Fahmy LM, et al. Individual case analysis of postmortem interval time on brain tissue preservation. *PLoS One* 2016; **11**: e0151615
- 48 Tariot PN, Lopera F, Langbaum JB, Thomas RG, Hendrix S, Schneider LS, et al. The Alzheimer's prevention initiative autosomal-dominant Alzheimer's disease trial: a study of Crenezumab versus placebo in preclinical PSEN1 E280A mutation carriers to evaluate efficacy and safety in the treatment of autosomal-dominant Alzheimer's disease, including a placebo-treated noncarrier cohort. *Alzheimer's Dement: Transl Res Clin Intervent* 2018; **4**: 150–60
- 49 Vandenberghe R, Rinne JO, Boada M, Katayama S, Scheltens P, Vellas B, et al. Bapineuzumab for mild to moderate Alzheimer's disease in two global, randomized, phase 3 trials. *Alzheimers Res Ther* 2016; **8**: 1–13
- 50 Salloway S, Honigberg LA, Cho W, Ward M, Friesenhahn M, Brunstein F, et al. Amyloid positron emission tomography and cerebrospinal fluid results from a Crenezumab anti-amyloid-beta antibody double-blind, placebo-controlled, randomized phase II study in mild-to-moderate Alzheimer's disease (BLAZE). *Alzheimers Res Ther* 2018; **10**: 96
- 51 Adolfsson O, Pihlgren M, Toni N, Varisco Y, Buccarello AL, Antonello K, et al. An effector-reduced anti- $\beta$ -amyloid (A $\beta$ ) antibody with unique A $\beta$  binding properties promotes neuroprotection and glial engulfment of A $\beta$ . *J Neurosci* 2012; **32**: 9677–89
- 52 Crespi GAN, Hermans SJ, Parker MW, Miles LA. Molecular basis for mid-region amyloid- $\beta$  capture by leading Alzheimer's disease immunotherapies. *Sci Rep* 2015; **5**: 9649
- 53 Miles LA, Crespi GA, Doughty L, Parker MW. Bapineuzumab captures the N-terminus of the Alzheimer's disease amyloid-beta peptide in a helical conformation. *Sci Rep* 2013; **3**: 1302
- 54 Hatami A, Albay R, Monjazeb S, Milton S, Glabe C. Monoclonal antibodies against A $\beta$ <sub>42</sub> fibrils distinguish multiple aggregation state polymorphisms in vitro and in Alzheimer disease brain. *J Biol Chem* 2014; **289**: 32131–43
- 55 Baghallab I, Reyes-Ruiz JM, Abulnaja K, Huwait E, Glabe C. Epitomic characterization of the specificity of the anti-amyloid A $\beta$  monoclonal antibodies 6E10 and 4G8. *J Alzheimers Dis* 2018; **66**: 1235–44

### Supporting information

Additional Supporting Information may be found in the online version of this article at the publisher's web-site:

**Figure S1.** Selectivity of 4G8 antibody using A $\beta$ <sub>x-40</sub> peptides.

**Figure S2.** Selectivity of 4G8 antibody using A $\beta$ <sub>x-42</sub> peptides.

**Figure S3.** Selectivity of different amyloid- $\beta$  antibodies.

**Figure S4.** Immunohistochemical staining of vascular and extracellular amyloid- $\beta$  peptides in a DS case (DS case 2).

**Figure S5.** Immunohistochemical staining of vascular and extracellular amyloid- $\beta$  peptides in a plaque-bearing nondemented control case (NDC case 11).

**Figure S6.** Immunohistochemical staining of vascular and extracellular amyloid- $\beta$  peptides in a nondemented control case (NDC case 6).

Received 31 January 2020

Accepted after revision 24 May 2020

Published online Article Accepted on 4 June 2020